



A Unified Height Reference System for Africa (AFRUHRS)

Mid-Term Report

Hussein A. Abd-Elmotaal

Minia University, Faculty of Engineering
Civil Engineering Department
Egypt
hussein.abdelmotaal@gmail.com

1. Overview

This report summarizes the main activities and achievements of the IUGG grant entitled “A Unified Height Reference System for Africa (AFRUHRS)”. The grant ran in the period 2020–2022. The lead applicant is IAG, represented by the IAG Secretary General, Markku Poutanen, Finnish Geospatial Research Institute FGI, National Land Survey of Finland. The Project Principal Participant of the IAG lead applicant is Hussein Abd-Elmotaal, Minia University, Egypt. The supporting applicant is IASPEI represented by the IASPEI Secretary General, Johannes Schweitzer, NOR SAR, Kjeller, Norway. The Project Principal Participant of the IASPEI supporting applicant is Rashad Kebeasy, National Research Institute of Astronomy and Geophysics, Egypt.

2. Activities and Achievements

A number of very important activities and tasks of the project have been achieved during the past period of the IUGG grant. They are summarized in the following sections.

2.1 Establishment of the Gravity Database of Africa (AFRGDB_V2.2)

The currently available gravity data are treated in somewhat different way to establish the AFRGRV_V2.2 gravity database for Africa. This treatment is described in the followings.

The currently available land gravity data set consists of 154,037 gravity data points. In order to enhance the behaviour of the empirical covariance function, the land data have



been filtered on a $1' \times 1'$ grid (i.e., in each cell of $1' \times 1'$, only one data point, the closest to the cell-center, has been selected). The number of land data after the grid filtering became 127,067 points.

The smart gross-error detection scheme developed by Abd-Elmotaal and Kührtreiber (2014) has been carried out on the land data set. That gross-error detection scheme uses the least-squares prediction technique. The gross-error detection technique estimates first the gravity anomaly value at the computational point using the values of the surrounding stations excluding the computational point. Comparing the estimated and data values defines a possible gross-error. Accordingly, the effect of the computational point on the surrounding stations is examined. Data points which show real gross-error behaviour are removed from the database. The number of land data after the gross-error removal became 126,202 points.

Figure 1 shows the distribution of the land data set (after grid filtering and gross-error removal). It illustrates that the land data still contain very large data gaps. The free-air gravity anomalies on land range between -163.2 mgal and 465.5 mgal with an average of about 9.8 mgal and a standard deviation of 40.9 mgal.

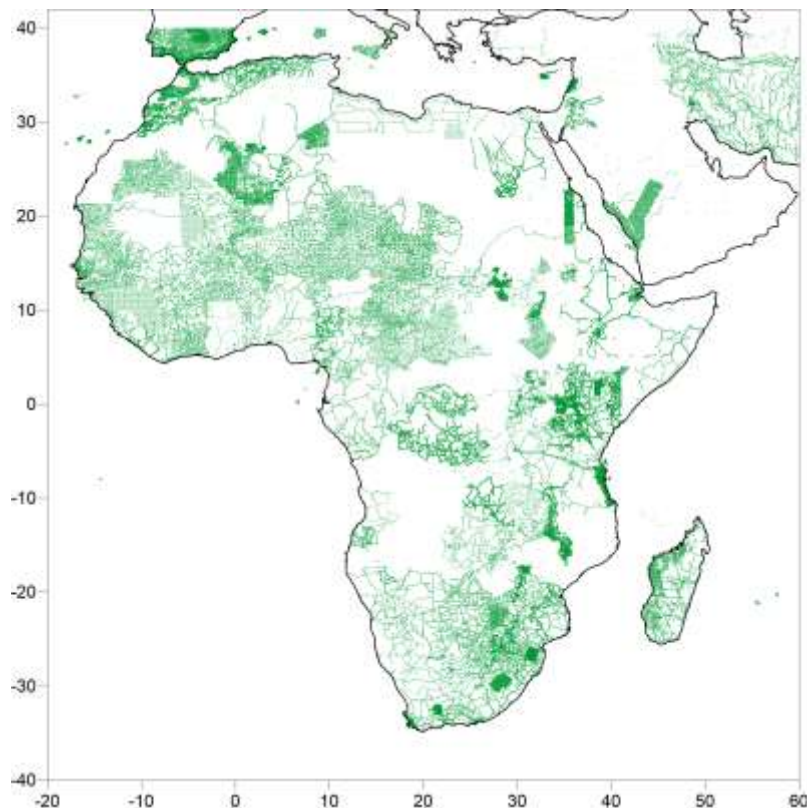


Fig. 1: Distribution of the land gravity data for Africa used to create the AFRGDB_V2.2 gravity database (after Abd-Elmotaal et al., 2020a).

The currently available shipborne gravity data set, after a preliminary gross-error detection scheme developed by Abd-Elmotaal and Makhloof (2013), consists of 971,945 gravity data points. The applied preliminary gross-error approach is based on the least-



squares prediction technique. It estimates the gravity anomaly value at the computational point using the values of the surrounding stations excluding the computational point. Hence, a comparison between the estimated and data values is used to define a possible blunder. The gross-error technique works in an iterative scheme till the standard deviation of the discrepancy between the data and estimated values is less than 1.5 mgal.

In order to enhance the behaviour of the empirical covariance function as well as to decrease the domination of the shipborne data, the shipborne data have been filtered on a $3' \times 3'$ grid. The number of shipborne data after the grid filtering became 148,858 points. A sophisticated gross-error detection scheme, similar to that applied on the land data (Abd-Elmotaal and Kühtreiber, 2014), has been carried out on the shipborne data set. The number of shipborne data after the sophisticated gross-error removal became 148,674 points.

Figure 2 shows the distribution of the shipborne gravity data (after grid filtering and gross-error removal). It illustrates a better distribution than that of the land data. The remaining gaps of the shipborne data are partially filled with the altimetry-derived gravity anomalies. The shipborne free-air gravity anomalies range between -238.3 mgal and 354.4 mgal with an average of about -6.2 mgal and a standard deviation of 34.9 mgal.

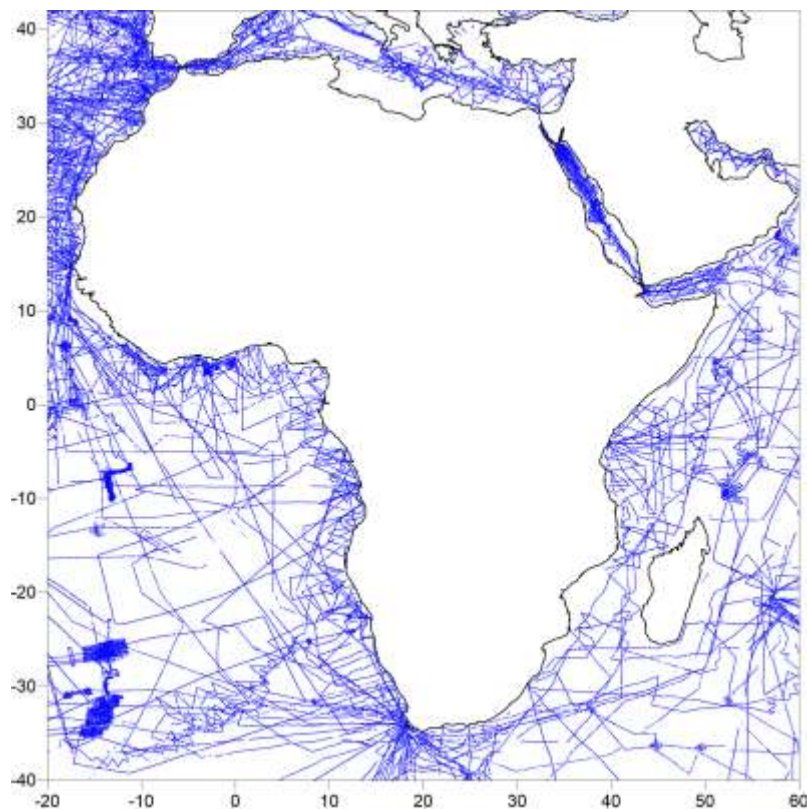


Fig. 2: Distribution of the shipborne gravity data for Africa used to create the AFRGDB_V2.2 gravity database (after Abd-Elmotaal et al., 2020a).

The currently available altimetry-derived gravity anomaly data set, which were constructed from the average of 44 repeated cycles of GEOSAT by the National Geophysical



Data Center NGDC (www.ngdc.noaa.gov), after applying a preliminary gross-error detection technique similar to that applied on the shipborne data, consists of 119,249 gravity data points. A combination between the shipborne and altimetry data took place. This combination causes some gaps along altimetry tracks when the altimetry data don't match with the shipborne data (cf. Fig. 3).

In order to enhance the behaviour of the empirical covariance function as well as to decrease the domination of the altimetry-derived data, the altimetry-derived data have been filtered on a $3' \times 3'$ grid. The number of altimetry-derived data after the grid filtering became 70,732 points. A sophisticated gross-error detection scheme, similar to that applied on the land data, has been carried out on the altimetry-derived data set. The number of altimetry-derived data after the sophisticated gross-error removal became 70,589 points.

Figure 3 shows the distribution of the available altimetry data (after grid filtering and gross-error removal). It illustrates, more or less, a regular distribution. The altimetry free-air gravity anomalies range between -172.2 mgal and 156.6 mgal with an average of 4.1 mgal and a standard deviation of 18.2 mgal.

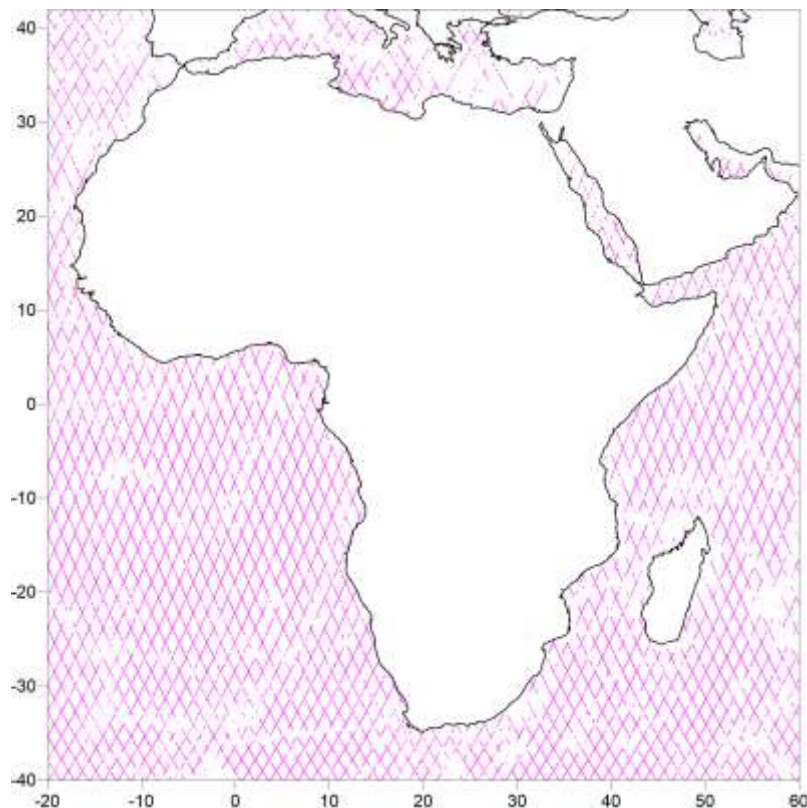


Fig. 3: Distribution of the altimetry gravity data for Africa used to create the AFRGDB_V2.2 gravity database (after Abd-Elmotaal et al., 2020a).

In order to reduce the free-mobility of the interpolation solution in the large data gaps, an underlying grid on a $15' \times 15'$ resolution has been created using the GOCE DIR-R5 model



complete to degree and order 300. A number of 48,497 underlying grid points have been created. Figure 4 shows the distribution of the underlying grid points. The underlying grid free-air gravity anomalies range between -175.1 mgal and 190.0 mgal with an average of 3.3 mgal and a standard deviation of 27.3 mgal.

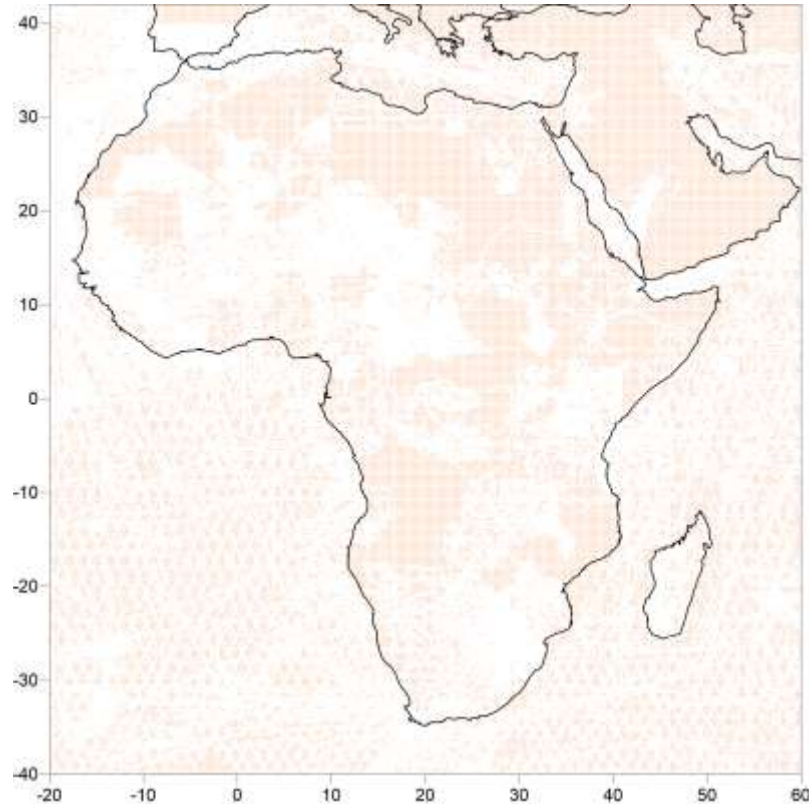


Fig. 4: Distribution of the underlying grid data for Africa used to create the AFRGDB_V2.2 gravity database (after Abd-Elmotaal et al., 2020a).

The residual terrain model (RTM) reduction technique (Forsberg, 1984) has been applied to reduce the gravity anomalies for Africa. The GOCE Dir_R5 model complete to degree and order 280 has been used. A study has been carried out to obtain the best smoothed reference surface needed for the RTM reduction. The reduced anomalies range between -140.33 mgal and 140.69 mgal with an average of 0.66 mgal and a standard deviation of 14.69 mgal.

An unequal weight least-squares interpolation technique takes place to interpolate the reduced gravity anomalies on a $5' \times 5'$ grid. The standard deviations of the different data sets have been taken as follows:

Gravity type	Std
Land	1 mgal
Shipborne	3 mgal
Altimetry	5 mgal



Underlying 20 mgal

Figure 4 shows the $5' \times 5'$ AFRGDB_V2.2 African free-air gravity anomaly database, after performing the RTM restore step. The free-air gravity anomalies range between -238.25 mgal and 511.98 mgal with an average of 3.19 mgal and a standard deviation of 31.86 mgal.

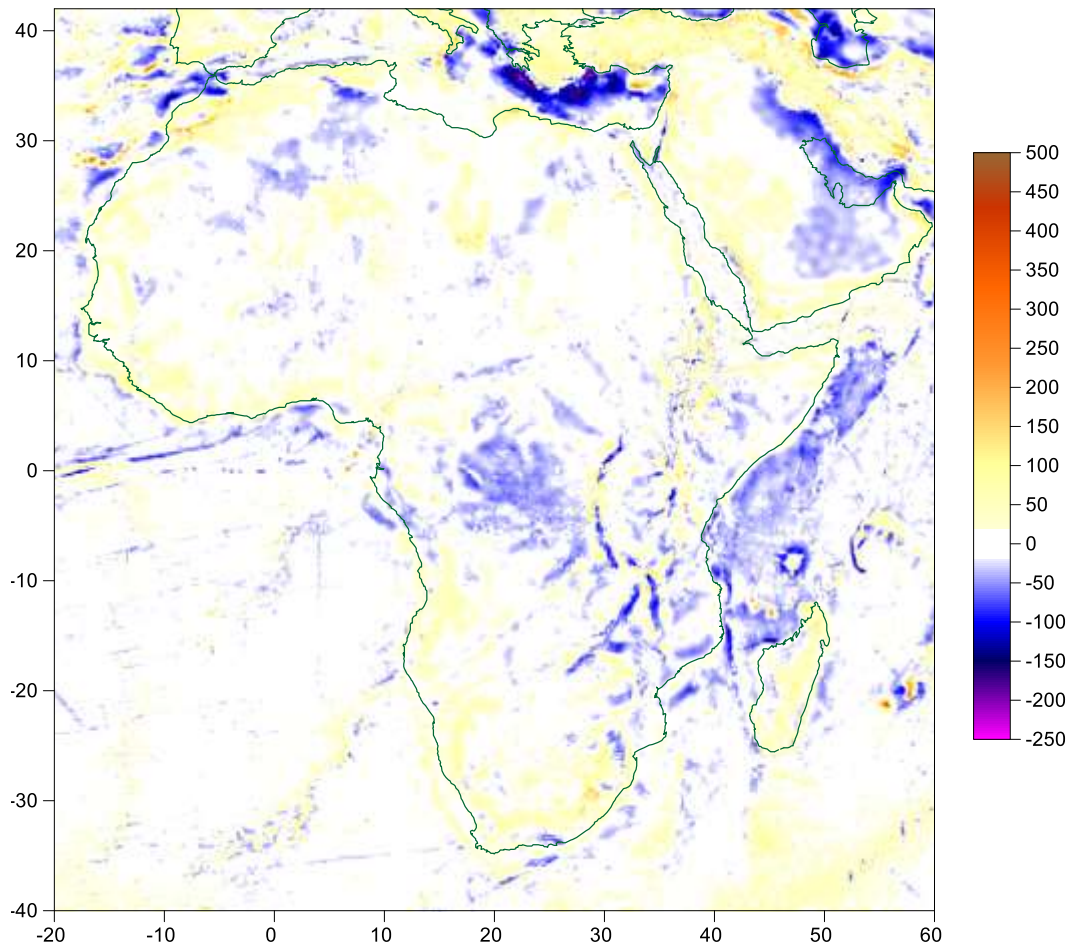


Fig. 4: The $5' \times 5'$ African free-air gravity anomaly database AFRGDB_V2.2 (after Abd-Elmotaal et al., 2020a). Units in [mgal].

As an estimation of the internal quality of the established free-air gravity anomaly database of Africa AFRGDB_V2.2, Fig. 5 shows the residuals between the measured and the database values at the data points used to create the database (those of Figs. 1, 2, 3). These residuals range between -51.09 mgal and 61.99 mgal with an average of -0.35 mgal and a standard deviation of 5.67 mgal. Figure 5 shows that most of the area (81.2% of the data points) have residuals below 5 mgal (the white pattern).

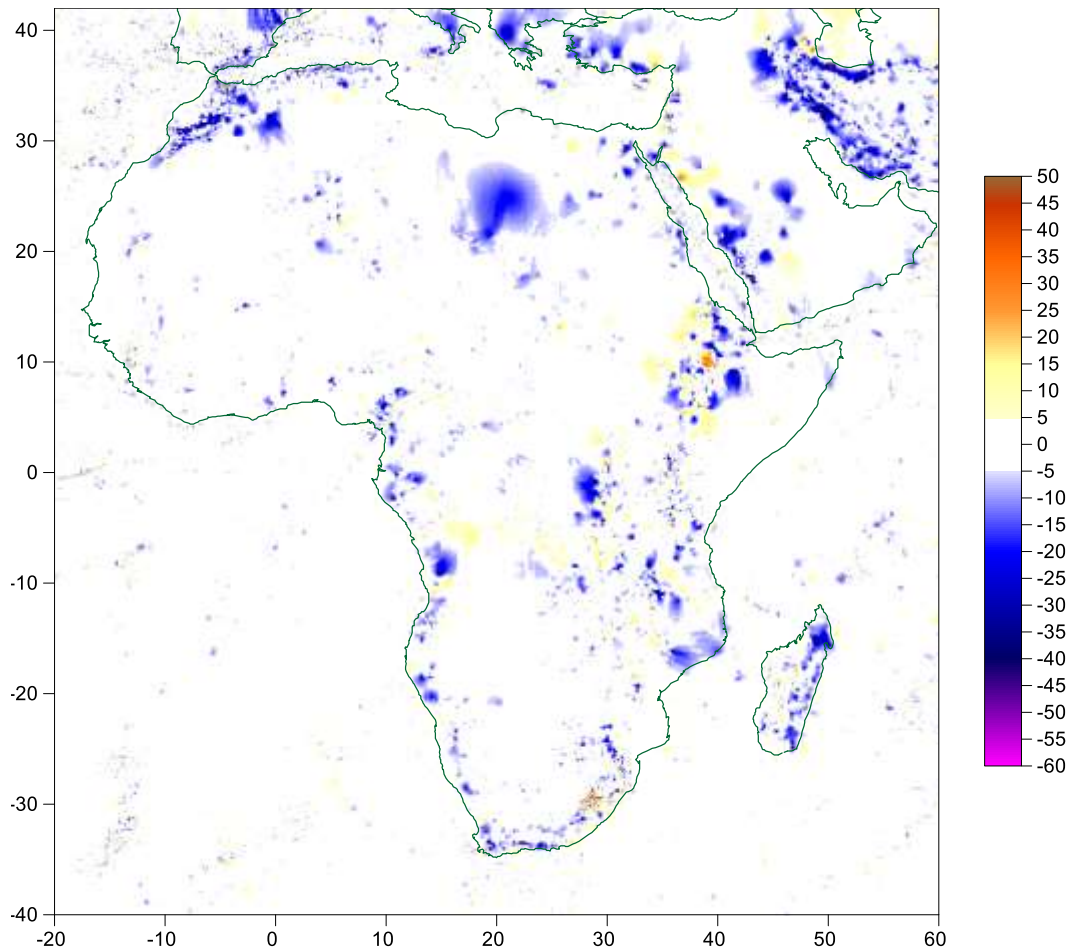


Fig. 5: Residuals at the data points between measured values and the $5' \times 5'$ African free-air gravity anomaly database AFRGDB_V2.2 (internal precision). Contour interval: 5 mgal (after Abd-Elmotaal et al., 2020a).

The external check of the AFRGDB_V2.2 has been estimated by comparing the values of the measured and database gravity anomalies for those points which were deselected by the grid-filtering technique (a set of around 898,000 points). Figure 6 shows the external check of the AFRGDB_V2.2 gravity database. These residual values range between -65.21 mgal and 65.10 mgal with an average of -0.59 mgal and a standard deviation of 7.27 mgal. Figure 6 shows that most of the area (69.1% of the data points) have residuals below 5 mgal (the white pattern).

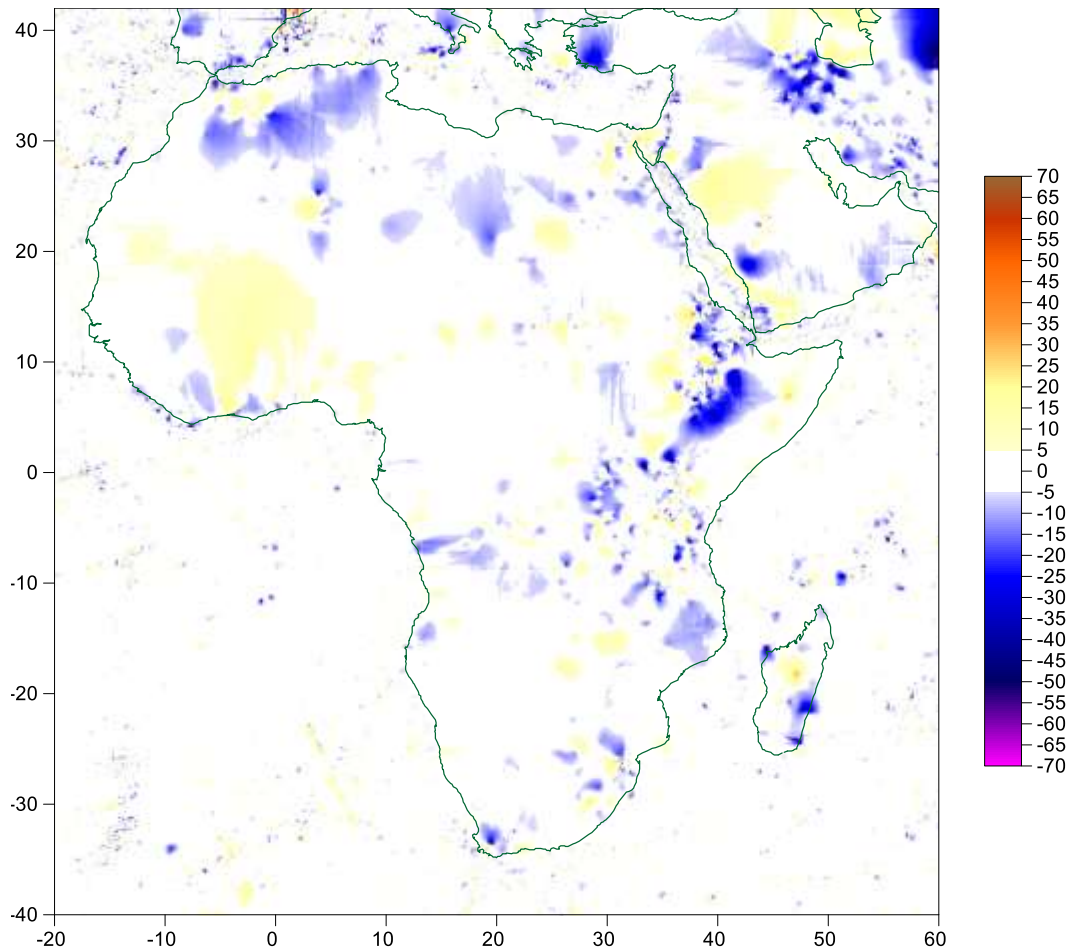


Fig. 6: Residuals at the points which were not used to create the database between measured values and the $5' \times 5'$ African free-air gravity anomaly database AFRGDB_V2.2 (external precision). Contour interval: 5 mgal (after Abd-Elmotaal et al., 2020a).

2.2 Effect of Qattara Depression

An approach appropriate to compute the effect of the land depressions on the gravity anomalies and geoid undulations when using the terrain reduction programs with unclassified digital terrain models (such as TC-program) has been developed by Abd-Elmotaal and Kühtreiber (2020). This approach depends on the unambiguous window remove-restore technique. The developed approach has successfully been applied to determine the effect of Qattara depression in Egypt on the gravity anomalies and geoid undulations.

The effect of Qattara depression on the gravity anomalies reaches 20 mgal and is located only at the area of the depression (cf. Fig. 7).

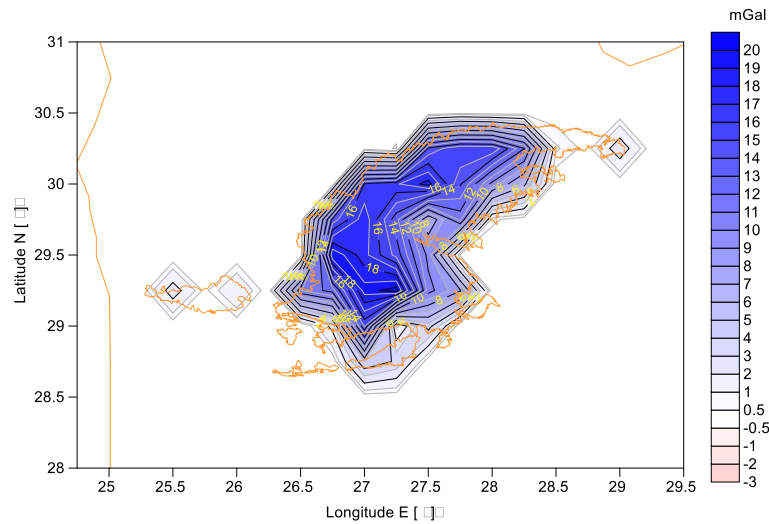


Fig. 7: Effect of Qattara Depression on the gravity anomalies (after Abd-Elmotaal and Kührtreiber, 2020).

The effect of Qattara depression on the geoid exceeds 1 m and is not only limited to the area of the depression but rather spreads out all over the whole country (in a radius of about 1000 km). This shows its significance and importance to be taken into account for a precise geoid determination.

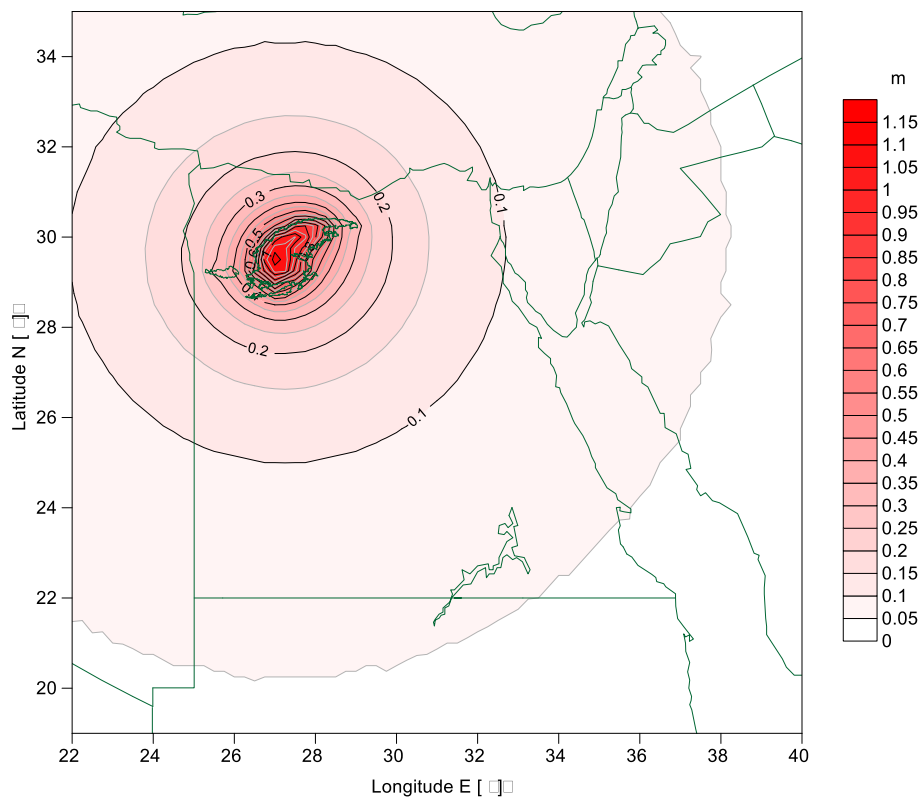


Fig. 8: Effect of Qattara Depression on the geoid undulation (after Abd-Elmotaal and Kührtreiber, 2020).



The indirect effect of Qattara depression on the geoid undulation is limited to the area of the depression and is below 1 dm. The contribution of the dimensionless harmonic coefficients of the topographic-isostatic masses of the data window equals the indirect effect for the Qattara depression. Accordingly they cancel out because of their opposite signs in the restore expression. Hence the total effect of Qattara depression on the geoid nearly equals the contribution of the gravity anomalies of Qattara depression on the geoid. Consequently, one may only compute the contribution of the gravity anomalies of the depression on the geoid representing the total effect of the depression on the geoid.

2.3 Effect of Great Lakes

The effect of great lakes on gravity reduction and geoid determination caused by unclassified DTMs for Africa has been studied (Abd-Elmotaal et al., 2020b). The case study is the Lake Victoria. The study proved that the great lakes have a significant effect on both gravity reduction and geoid undulations, and hence they have to be considered for precise geoid determination.

Figure 9 illustrates the effect of Lake Victoria on the gravity reduction. It shows that this effect is almost confined to the area of the lake with positive effect inside the lake reaching approximately 4 mgal and negative effect just outside the border of the lake reaching only -1.6 mgal.

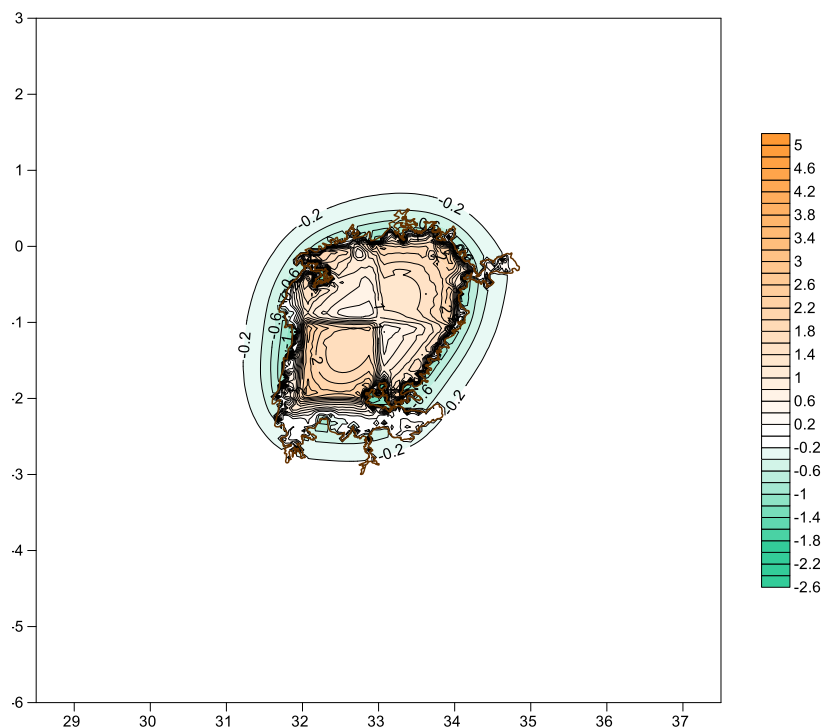


Fig. 9: Effect of Lake Victoria on the gravity reduction. Units are in [mgal] (after Abd-Elmotaal et al., 2020b).



Figure 10 illustrates the effect of Lake Victoria on the geoid undulation. It shows that the total effect of the topographic-isostatic masses of the lake on the geoid undulation is nearly isotropic, reaches about 28 cm and decreases with radial distance.

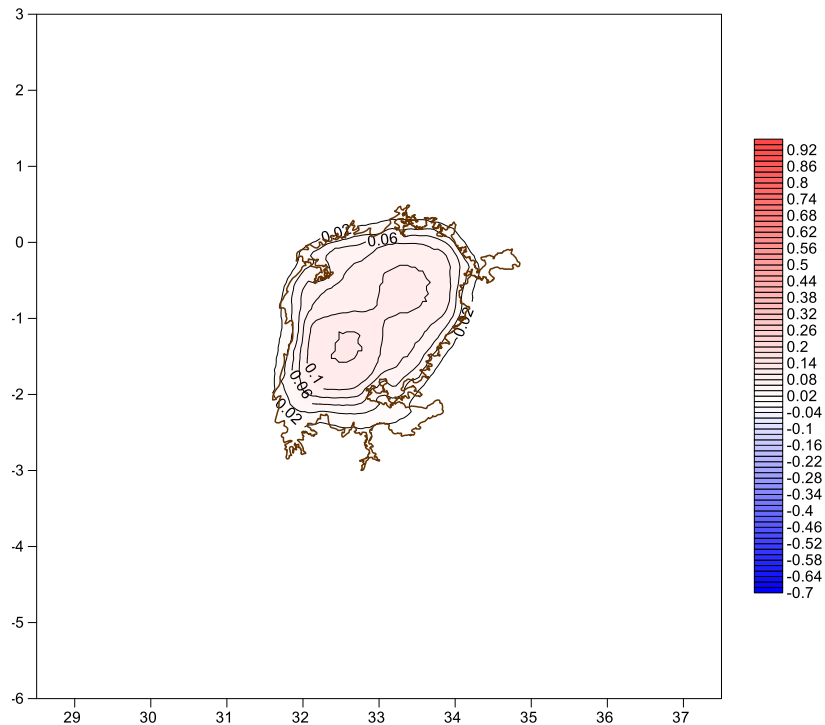


Fig. 10: Effect of Lake Victoria on the geoid undulation. Units are in [m] (after Abd-Elmotaal et al., 2020b).

2.4 Improving the Accuracy of the Harmonic Analysis of the Window Topographic-Isostatic Masses

In the context of the window remove-restore technique (Abd-Elmotaal and Kühtreiber, 2003), the harmonic analysis of the window topographic-isostatic masses represents an important issue. As the developed earth models are recently available to an ultra-high degree, the harmonic analysis of the window topographic-isostatic masses should also be carried out to that ultra-high degree. New set of rigorous expressions utilizing the ellipsoid geometry has been developed and tested by Abd-Elmotaal and Kühtreiber (2021a).

Figure 11 shows a comparison between the degree variances of the global topographic–isostatic potential utilizing the new developed ellipsoidal expressions compared to those using the 2003-spherical expressions. Figure 11 shows clearly that the old spherical expressions (Abd-Elmotaal and Kühtreiber 2003) produce significantly higher power spectrum, especially for higher degrees. This is why these old spherical expressions cannot be used for the harmonic analysis of the topographic–isostatic masses up to ultra-high degrees.

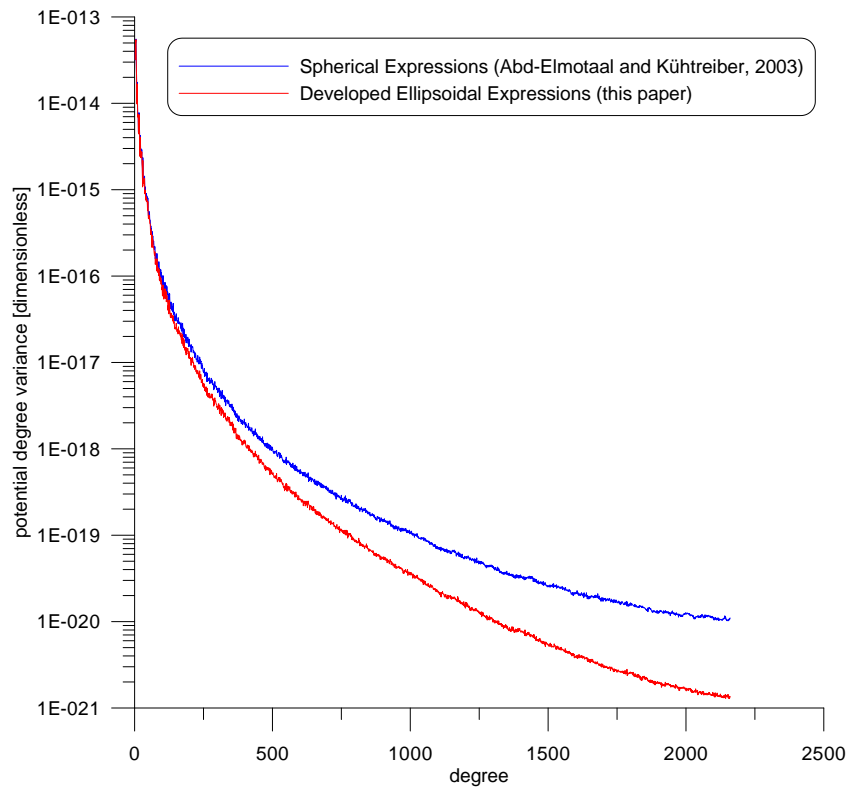


Fig. 11: Degree variances of the global topographic–isostatic potential utilizing the 5'×5' SRTM DTM and the Airy–Heiskanen isostatic model (after Abd-Elmotaal and Kühtreiber, 2021a).

Figure 12 illustrates the dimensionless potential degree variances of the four models: `dV_ELL_RET2012`, `RWI_TOPO_2015`, `ROLI_EllApprox_SphN_3660` and the model generated by the proposed technique with the developed ellipsoidal expressions. Figure 12 shows clearly that they match to a great extent. It should, however, be mentioned that for the four harmonic models, different topographic models have been used, which is likely responsible for the slight mismatching between the harmonic models at the ultra-high degrees.

The local tests proved that the window-reduced anomalies employing the proposed technique for computing the harmonic analysis of the local topographic-isostatic potential to an ultra-high degree are smooth and having a drastically small variance, even for high mountainous regions.

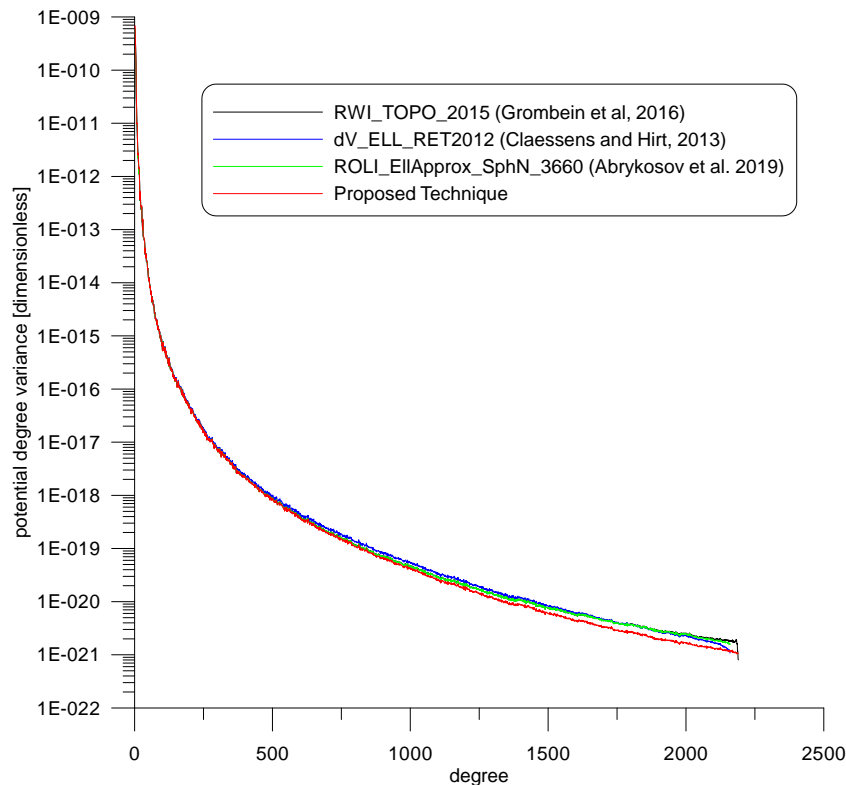


Fig. 12: Degree variances of the global topographic–isostatic potential utilizing the 5'×5' SRTM DTM and the Airy–Heiskanen isostatic model (after Abd-Elmotaal and Kühtreiber, 2021a).

The main advantage of the present developed technique, compared to existing alternative techniques, is that it can be used to compute the harmonic analysis of the topographic-isostatic potential for a certain data window or for the whole earth. The approach is a direct one, i.e., it computes the harmonic analysis of the topographic-isostatic potential directly from the masses themselves. Only a very small approximation has been implemented within the derivation process of the developed expressions, namely that the ellipsoidal normal coincides with the radius vector.

It is worth mentioning that the very smooth window-reduced anomalies, achieved by applying the proposed technique with the developed ellipsoidal expressions for computing the harmonic analysis of the local topographic-isostatic potential to an ultra-high degree, are well suited for all geodetic applications, such as gravity interpolation and geoid determination.

It is important to mention that the developed technique has neither a theoretical nor numerical limitations in terms of the resolution of the used DTM nor the upper ultra-high degree of the spherical harmonic expansion. However, one should keep in mind that the solution is done as a numerical integration and consequently, the larger the number of pixels of the used DTM and/or the larger the ultra-high maximum degree of the wanted harmonic expansion, the larger is the needed CPU time. A cluster computation would thus offer itself in that case.



2.5 An Alternative Geoid Model for Africa using the Shallow-Layer Method

An alternative geoid model for Africa using the shallow-layer method has been determined by Ashry et al. (2021). The shallow-layer method, following the basic definition of the geoid, differs essentially from the traditional geoid determination techniques (Stokes and Molodensky) that it doesn't need real gravity data. It comes from the definition of the geoid. Here, the shallow-layer method is used to determine a $5' \times 5'$ geoid model for Africa. The earth gravitational model (EGM2008), the global topographic model (DTM2006.0), the global crustal model (CRUST1.0) and the Danish National Space Center data set (DNSC08) global models have been used to construct and define the shallow layer and its interior structure. A combination of prism and tesseroid modelling methods have been utilized to determine the gravitational potential produced by the shallow-layer masses. The validation and tests of the computed shallow-layer geoid have been done at two different levels. First, a comparison between the computed shallow-layer geoid and the recently developed AFRgeo2019 gravimetric geoid for Africa based on real gravity data (Abd-Elmotaal et al., 2020c) has been carried out. Second, a comparison of the computed shallow-layer geoid with several geoid models computed using different global geopotential models has been performed. The results show that the computed shallow-layer geoid behaves similarly to those determined by the global geopotential models. Differences between the shallow-layer and the AFRgeo2019 gravimetric geoids are generally small (below 0.5 m) at most of the African continent.

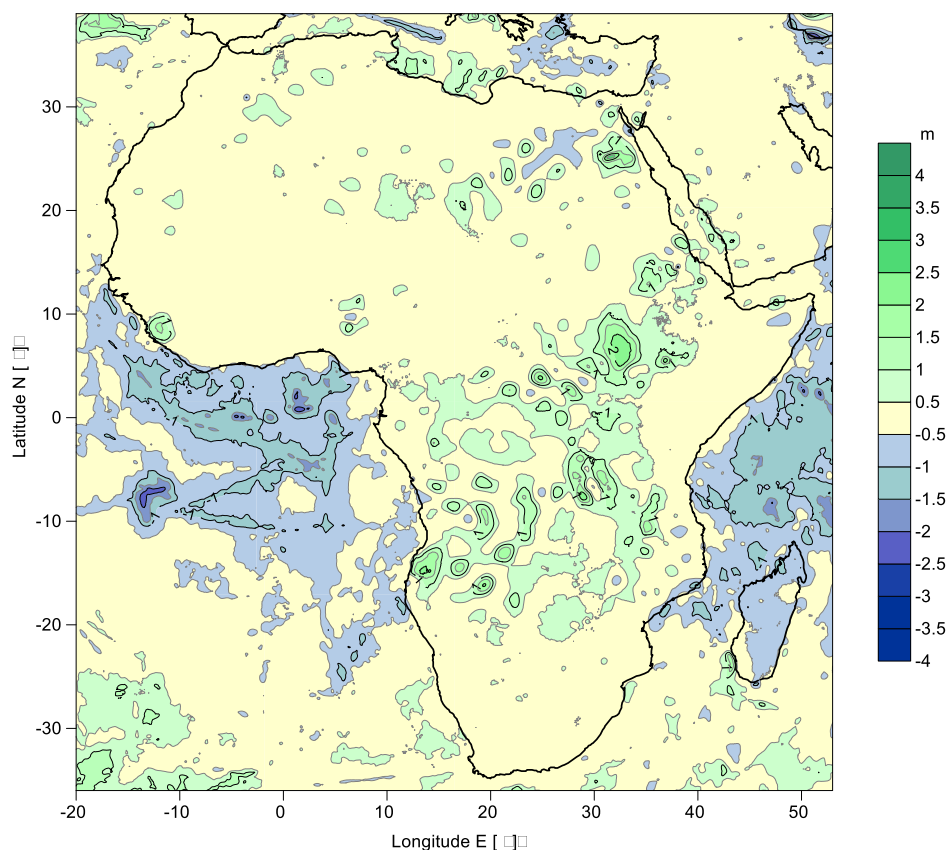


Fig. 13: Difference between the shallow-layer and ARgeo2019 geoid models for Africa (after Ashry et al., 2021).



2.6 Validation of Using SWARM to Fill-in the GRACE/GRACE-FO Gap: Case Study in Africa

The American/German missions Gravity Recovery and Climate Experiment (GRACE) and the GRACE Follow-On (GRACE-FO) and the European mission (Swarm) play an important role for study the Earth's gravity field with unprecedented high-precision and high-resolution measurements. A study to use Swarm data to fill-in the data-gap between GRACE and GRACE-FO missions from July 2017 to May 2018 has been conducted by Mohasseb et al. (2021). Africa has been chosen as the study area. We used the available data from the triple GRACE processing centers CSR, GFZ and JPL, in addition to the Swarm TVGF data provided by the Czech Academy of Sciences (ASU) and the International Combination Service for Time-variable Gravity (COST-G). The GRACE and Swarm data have been tested in the frequency and space domains. For the frequency domain, the data assessed in two different levels: the potential degree variances and the harmonic coefficients themselves. The results show consistency between GRACE/GRACE-FO and Swarm for all processing centers. In the space domain, a comparison between GRACE/GRACE-FO and Swarm for the Terrestrial Water Storage (TWS), gravity anomaly, and the potential/geoid have been carried out. The results indicated that a fully agreement between all processing centers for GRACE and Swarm in the potential degree variances in the frequency domain in addition gravity anomaly and the geoid undulation in space domain, while it shows a significant different in the harmonic coefficients themselves and TWS in frequency and space domain respectively. Eventually, we use the parametric least square adjustment to estimate the new Swarm-modified coefficients, and we chose Swarm ASU and GRACE and GRACE-FO CSR data in order to be used in our processing. The new coefficients made exceedingly agreement between the original GRACE coefficient and the new coefficients in all aspects.

Figure 14 shows the geoid undulation for Africa computed using GRACE and SWARM models. It shows a great agreement between the used models.

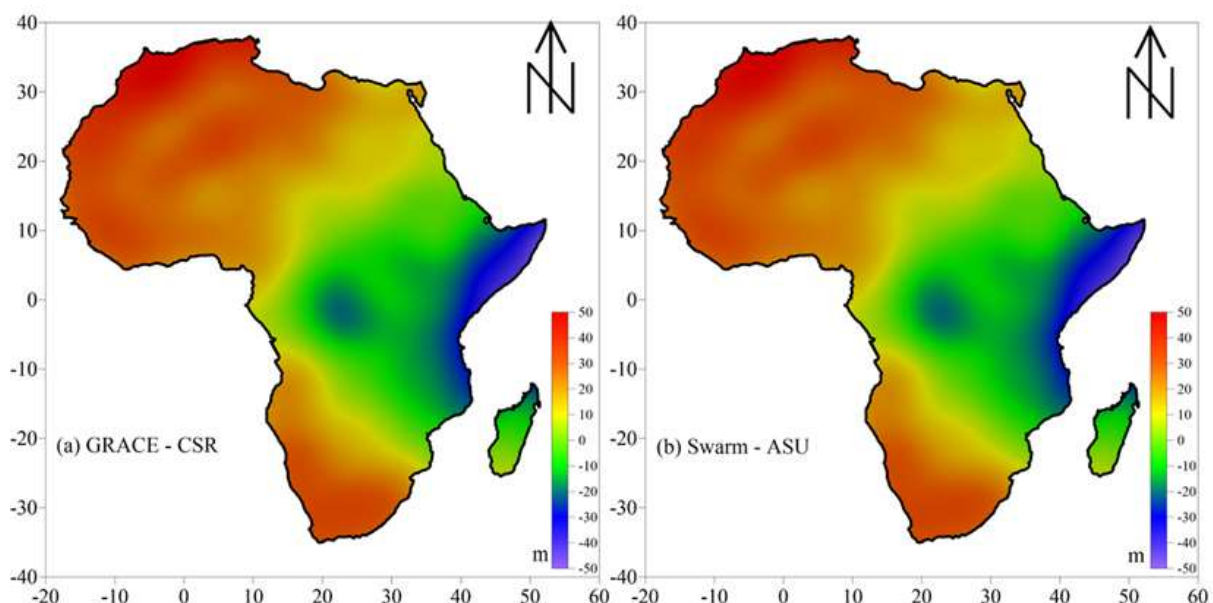


Fig. 14: Geoid undulation for Africa computed using GRACE and SWARM models (after Mohasseb et al., 2021).



2.7 Optimum DHM Resolution for the Window Remove-Restore Technique

A study aiming to determine the optimum DHM resolution for the window remove-restore technique has been carried out for Africa by Abd-Elmotaal and Kühtreiber (2021b). First a local study on Morocco/Atlas mountain area has been conducted and it proved that the 30"×30" DHM gives practically the same results as the most fine 3"×3" DHM. Accordingly, a regional study for the African continent took place to test the difference between the 30"×30" DHM and other coarser DHMs. Figure 15 illustrates the harmonic analysis difference between the 30"×30" DHM and other coarser DHMs for Africa. It shows that neither the 3'×3' nor the 5'×5' DHMs can be used to generate the window topographic-isostatic harmonic coefficients, as they give quite high differences. Using the 30"×30" DHM is optimum and it needs 142 days of CPU time compared to 14200 days for the most fine 3"×3" DHM. The 1'×1' DHM gives reasonable accuracy in 36 days of CPU time.

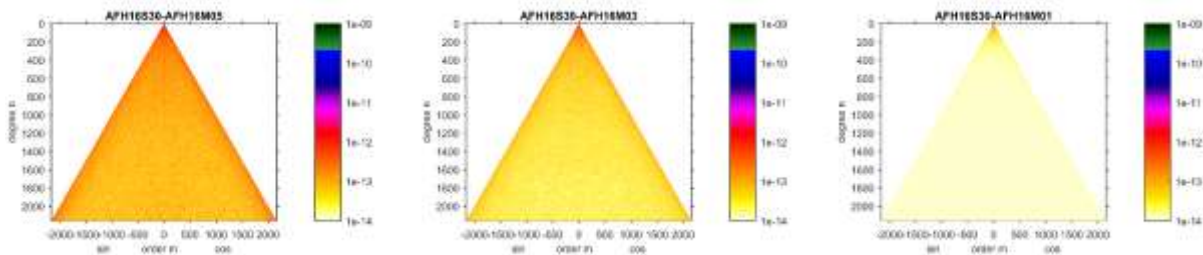


Fig. 15: Harmonic analysis difference between the 30"×30" DHM and other coarser DHMs for Africa (after Abd-Elmotaal and Kühtreiber, 2021b).

The effect in the space domain for the gravity anomaly is illustrated in Fig. 16. The 5'×5' DHM gives difference between -48 to 62 mgal with a standard deviation of about 2 mgal. The 3'×3' DHM gives difference between -13 to 28 mgal with a standard deviation of about 0.66 mgal. While, the 1'×1' DHM gives difference between -1.5 to 2.1 mgal with a standard deviation of only 0.06 mgal. This immediately shows that the 1'×1' DHM can do the job within significantly less CPU time.

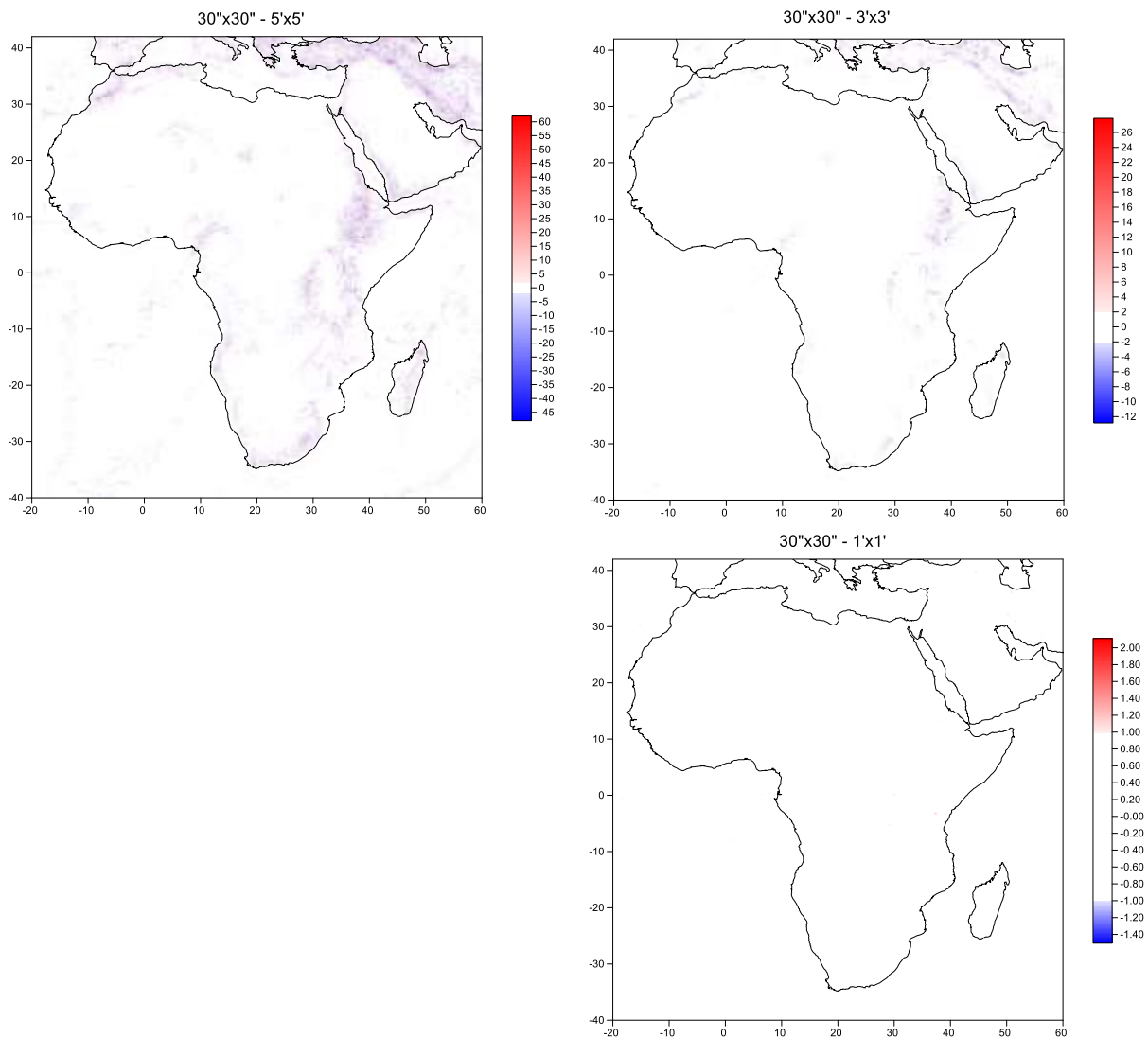


Fig. 16: Gravity anomaly difference between the 30''x30'' DHM and other coarser DHMs for Africa. Units in [mgal] (after Abd-Elmotaal and Kühtreiber, 2021b).

The effect in the space domain for the geoid undulation is illustrated in Fig. 17. The 5'x5' DHM gives difference between -15 to 34 cm with a standard deviation of about 1 cm. The 3'x3' DHM gives difference between -4 to 12 cm with a standard deviation of about 0.35 mgal. While, the 1'x1' DHM gives difference between -0.3 to 1.2 cm with a standard deviation of only 0.05 cm. This shows again that the 1'x1' DHM can do the job within significantly less CPU time.

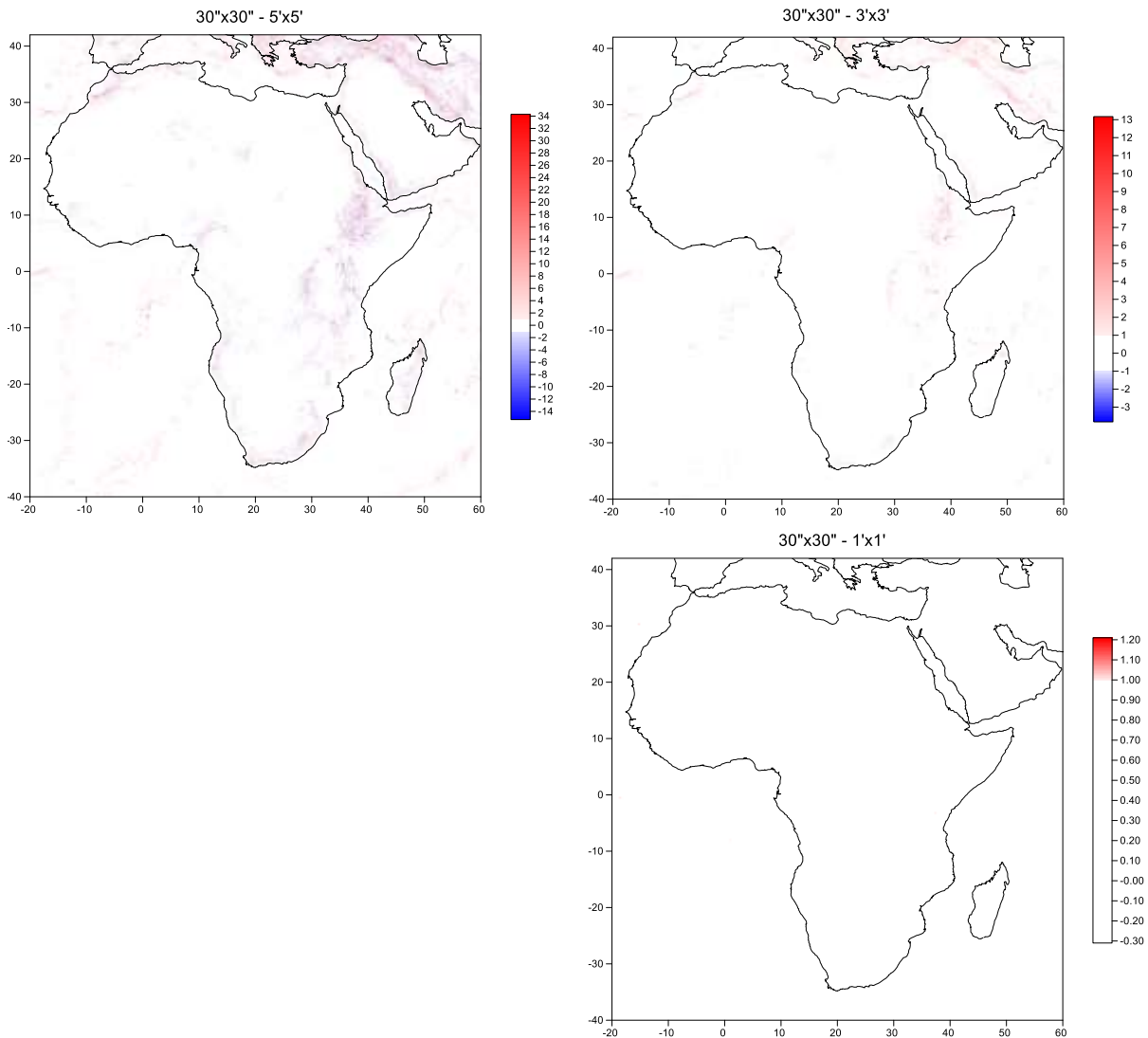


Fig. 17: Geoid undulation difference between the 30'' \times 30'' DHM and other coarser DHMs for Africa. Units in [cm] (after Abd-Elmotaal and Kührtreiber, 2021b).

3. Future Activities

- Developing an optimal terrain correction software for window remove-restore technique suitable for the huge size of Africa in order to reduce the needed CPU time. This study is going to be presented online in the AGU Fall Meeting, AGU2021 (December 13-17, 2021), New Orleans, USA.
- A study on the effect of the gravity data coverage on the gravity field recovery, especially for the large data gaps as the case for Africa.
- A study on the evaluation of the AFRGDB_V2.0 and AFRGDB_V2.2 African gravity databases.



- Generating a detailed gravity database for the determination of a unified height reference system for Africa with the possibility to utilize the variable crustal density.

The above activities are aimed (hopefully) to be presented in the following international conferences (or at least two of which):

- EGU2022 (April 3 - 8, 2022), Vienna, Austria.
- Hotine/Marrusi (June 13-17, 2022), Milan, Italy.
- GGHS2022 (September 12-17, 2022), Austin, USA.

4. Effect on the COVID-19 Pandemic

- Preventing traveling to international conferences, and hence miss the valuable feedback from peers.
- Reducing the collaboration between the international scholars in the context of the IUGG grant project.
- Precautions connected with meetings, discussions, collaborating at the national level.

5. Publications

A number of papers are published within the course of the project. Here follows a list of these publications among other references cited in this report.

1. Abd-Elmotaal, H. and Kühtreiber, N. (2021a) Direct Harmonic Analysis for the Ellipsoidal Topographic Potential with Global and Local Validation. *Surveys in Geophysics*, Vol. 42, 159–176, <https://doi.org/10.1007/s10712-020-09614-4>.
2. Abd-Elmotaal, H. and Kühtreiber, N. (2021b) On the Optimum DHM Resolution for the Window Remove-Restore Technique: Case Study for Africa. Scientific Assembly of the International Association of Geodesy, Beijing, China, June 28 – July 2, 2021.
3. Abd-Elmotaal, H. and Kühtreiber, N. (2020) Effect of Qattara Depression on Gravity and Geoid Employing Unclassified Digital Terrain Models. *Studia Geophysica et Geodaetica*, Vol. 64, 186–201, <https://doi.org/10.1007/s11200-018-1240-x>.
4. Abd-Elmotaal, H. and Kühtreiber, N. (2014) Automated Gross Error Detection Technique Applied to the Gravity Database of Africa. General Assembly of the European Geosciences Union (EGU), Vienna, Austria, April 27 – May 2, 2014.
5. Abd-Elmotaal, H. and Kühtreiber, N. (2003) Geoid Determination Using Adapted Reference Field, Seismic Moho Depths and Variable Density Contrast. *Journal of Geodesy*, Vol. 77, 77–85, DOI: 10.1007/s00190-002-0300-7.



6. Abd-Elmotaal, H., Kühtreiber, N., Seitz, K. and Heck, B. (2020a) The New AFRGDB_V2.2 Gravity Database for Africa. *Pure and Applied Geophysics*, Vol. 177(9), 4365–4375, <https://doi.org/10.1007/s00024-020-02481-5>.
7. Abd-Elmotaal, H., Seitz, K., Ashry, M. and Heck, B. (2020b) Effect of Great Lakes on Gravity Reduction and Geoid Determination Caused by Unclassified DTMs: Case Study for Lake Victoria, Africa. *Journal of Geodesy*, Vol. 94, <https://doi.org/10.1007/s00190-020-01410-7>.
8. Abd-Elmotaal, H., Kühtreiber, N., Seitz, K. and Heck, B. (2020c) A Precise Geoid Model for Africa: AFRgeo2019. *International Association of Geodesy Symposia*, https://doi.org/10.1007/1345_2020_122.
9. Abd-Elmotaal, H. and Makhloof, A. (2013) Gross-Errors Detection in the Shipborne Gravity Data Set for Africa. *Geodetic Week, Essen, Germany, October 8–10, 2013* (http://www.uni-stuttgart.de/gi/research/Geodaetische_Woche/2013/session02/Abd-Elmotaal-Makhloof.pdf).
10. Mohasseb, H., Abd-Elmotaal, H. and Shen, W. (2021) Validation of Using SWARM to Fill-in the GRACE/GRACE-FO Gap: Case Study in Africa. *General Assembly of the European Geosciences Union (EGU), Vienna, Austria, April 19 – 30, 2021*.
11. Ashry, M., Shen, W. and Abd-Elmotaal, H. (2021) An alternative geoid model for Africa using the shallow-layer method. *Studia Geophysica et Geodaetica*, Vol. 65, 148–167, <https://doi.org/10.1007/s11200-020-0301-0>.